

Quantum rate constants for the $\text{H}_2 + \text{OH}$ reaction with the centrifugal sudden approximation

Dong H. Zhang

Department of Computational Science, National University of Singapore, Singapore, 119260

John C. Light

Department of Chemistry and The James Franck Institute, The University of Chicago, Chicago, Illinois 60637

Soo-Y. Lee

Department of Chemistry, National University of Singapore, Singapore, 119260

(Received 3 March 1998; accepted 26 March 1998)

The cumulative reaction probability (CRP) has been calculated for the $\text{H}_2 + \text{OH} \leftrightarrow \text{H}_2\text{O} + \text{H}$ in its full dimensionality by using the centrifugal sudden (CS) approximation for $J > 0$. The Boltzmann average of the CRP provides the most accurate thermal rate constant to date for the title reaction on the Walch, Dunning, Schatz, Elgersma (WDSE) potential energy surface (PES). It is found that the theoretical rate is larger than the experimental value in the low temperature region (a factor of ~ 1.8 at 300 K), and smaller than the experimental value for temperatures higher than 500 K, indicating that a more accurate PES is needed to provide a quantitative description of the title reaction. We also demonstrate that the "J-shifting" approximation in which we calculate $N(J > K, K)$ from $N(J = K, K)$ by an energy shift works very well for this reaction. However, the "J- and K-shifting" approximation [calculating $N(J, K)$ from $N(J = 0, K = 0)$] overestimates the rate for this reaction by about 60% for all the temperatures investigated. It is also found that the CS rate constant is substantially lower than the rate constant for the ground rovibrational state of the reagents calculated on the same PES, indicating that initial rotational excitation is important to the thermal rate constant for this reaction (it causes a decrease). © 1998 American Institute of Physics.
[S0021-9606(98)02025-X]

I. INTRODUCTION

Significant progress has been made in the last few years in quantum reactive scattering studies of four-atom reactions in the gas-phase. Starting from reduced dimensionality approaches,^{1,2} it is now possible to carry out full-dimensional quantum calculations for diatom-diatom³⁻⁵ and atom-triatom⁶ reactions due to the development of new theoretical and computational methodologies and the exploitation of increasingly fast computers. Accurate quantum scattering studies have been carried out for a number of important four atom reactions, such as the $\text{H}_2 + \text{OH} \leftrightarrow \text{H}_2\text{O} + \text{H}$ ^{3,4,6-8} and its isotopically substituted reactions,⁹⁻¹¹ the $\text{HO} + \text{CO}$ reaction,¹² and recently the $\text{H}_2 + \text{CN}$ reaction.¹³ Total reaction probabilities, cross sections, rate constants, and even final state resolved reaction probabilities have been reported for these reactions for a few initial states. The cumulative reaction probabilities (CRP) $N(E)$ for $J=0$ have also been calculated for the $\text{H}_2 + \text{OH}$ ¹⁴⁻¹⁶ and $\text{H}_2 (\text{D}_2) + \text{CN}$ ¹⁷ reactions. These studies provide unprecedented quantitative descriptions of these four-atom reactions.

However, these earlier quantum results are still not sufficient to be used for unambiguous comparisons with experimental observations, or to judge conclusively the quality of the potential energy surface (PES) used in dynamics calculation. For example, in order to compare with the experimen-

tal thermal rate constants, the "J- and K-shifting" approximation^{18,19,1} was invoked earlier to obtain the theoretical rate constants from the CRP for $J=0$.^{14,15} (The CRP's for $J > 0$ are extremely demanding computationally.) The J-shifting and K-shifting approximations are both based on the assumption that the total angular momentum J and its projection on the body-fixed axis K only affect on the reaction probability by an energy shift due to the effective rotational potential at the transition state.^{18,19} These approximations have never been tested for a four-atom reaction. A recent study on triatom systems showed that the variation of K has a stronger effect on the dynamics than the change of J because it affects more strongly the internal motions.²⁰ Thus we should treat rate constants obtained by using the J- and K-shifting approximation for four-atom reactions with caution. One purpose of this study is to evaluate the adequacy of these approximations.

Some time ago, we developed the transition state wave packet method (TSWP)²¹ to calculate efficiently the cumulative reaction probabilities $N(E)$ at all energies desired from a single propagation of each transition state wave packet forward and backward in time. The $N(E)$'s so obtained can then be thermally averaged to produce the thermal rate constants at all desired temperatures. This approach differs from the other approaches to calculating either the rate constant²²⁻²⁶ or $N(E)$ ^{27,14} directly in that we do not have to repeat our time dependent calculations for different energies

or temperatures. The great efficiency of the new method for direct reactions, demonstrated on the $\text{H}_2 + \text{OH}$ reaction¹⁶ and recently on the $\text{H}_2 (\text{D}_2) + \text{CN}$ reaction,¹⁷ makes it possible to carry out the calculation of the total CRP $N(E)$ summed over all important angular momentum values J for some four atom reactions.

In this paper, we report the first calculation of $N(E)$ for a four-atom reaction summed over J . Specifically, we present the full dimensional quantum calculations of CRP $N(E)$ for the reaction of $\text{H}_2 + \text{OH}$ under the centrifugal sudden (CS) approximation.^{28,29} We use the WDSE PES^{30,31} modified by Clary.³² From these $N(E)$'s one can obtain the thermal rate constants via the Boltzmann average. Although the CS approximation also has not been tested for any four-atom reaction, it has been tested for some atom-diatom reactions, and found to be within 20%–25% of the accurate thermal rate constant. A recent test by Aguado³³ showed the CS approximation works very well for the $\text{Li} + \text{HF}$ reaction, while another recent test by Miller and co-workers revealed that it is not very accurate for the $\text{Cl} + \text{H}_2$ reaction (although they did not show how bad the CS rate constant is compared to their accurate result).²⁶ However, it is generally accepted that the CS approximation is more reliable than the J- and K-shifting approximation for most reactions. Thus we believe that our calculation should provide the most accurate rate constant for this four atom reaction to date as well as a rather unambiguous test for the accuracy of the PES and the validity of J- and K-shifting approximation for this four-atom reaction. This study not only demonstrates our ability to accurately calculate rate constants for four-atom reactions on a given potential energy surface, it is also of practical importance for modeling this very important combustion and atmospheric reaction.

The paper is organized as follows: In Sec. II we outline the theoretical methodology of the TSWP approach to $N(E)$ for the $\text{H}_2 + \text{OH}$ reaction. Section III presents the results of our calculation, including $N(E)$ and rate constants for the title reaction as well as comparisons with the J-shifting and J- and K-shifting approximations. We conclude in Sec. IV.

II. THEORY

A. The TSWP approach to $N(E)$

The transition state wave packet (TSWP) approach to the CRP $N(E)$ was derived by Zhang and Light²¹ from the well-known formulation given by Miller and co-workers,³⁴

$$N(E) = \frac{(2\pi)^2}{2} \text{tr}[\delta(E-H)F_2\delta(E-H)F_1], \quad (1)$$

where the F_i 's are quantum flux operators at dividing surfaces i (which may or may not be the same)

$$F = \frac{1}{2\mu} [\delta(q-q_0)\hat{p}_q + \hat{p}_q\delta(q-q_0)]. \quad (2)$$

Here μ is the reduced mass of the system, q is the coordinate perpendicular to the dividing surface located at $q=q_0$ which separates products from reactants, and \hat{p}_q is the momentum operator conjugate to the coordinate q . It is well known that in one dimension the flux operator is of rank two with only a

\pm pair of nonvanishing eigenvalues. The corresponding eigenstates are also complex conjugates,^{22,23,35}

$$F|\pm\rangle = \pm\lambda|\pm\rangle. \quad (3)$$

In the TSWP approach we first choose a dividing surface \mathbf{S}_1 separating the products from reactants preferably located to minimize the density of internal (transition) states for the energy region considered. The initial transition state wave packets $|\phi_i^+\rangle$ ($i=1,n$) are constructed as the direct products of the Hamiltonian eigenstates on \mathbf{S}_1 , $|\phi_i\rangle$, and flux operator eigenstate $|+\rangle$ with positive eigenvalue λ for the coordinate perpendicular to \mathbf{S}_1 , i.e.,

$$|\phi_i^+\rangle = |\phi_i\rangle|+\rangle \quad \text{with} \quad H_{\mathbf{S}_1}|\phi_i\rangle = \varepsilon_i|\phi_i\rangle. \quad (4)$$

The trace in Eq. (1) then can be efficiently evaluated in terms of $|\phi_i^+\rangle$ ($i=1,n$). Utilizing the Fourier transform identity between the energy and time domains for $\delta(E-H)$, we convert the problem into a time-dependent one by propagating $|\phi_i^+\rangle$ ($i=1,n$) in time as in the initial state selected wave packet approach to get the cumulative reaction probability $N(E)$,

$$N(E) = \sum_{i=1}^n N_i(E) = \sum_{i=1}^n \langle \psi_i(E) | F | \psi_i(E) \rangle. \quad (5)$$

The energy-dependent wave functions $|\psi_i(E)\rangle$ are calculated on the second dividing surface as

$$\psi_i(E) = \sqrt{\lambda} \int_{-\infty}^{+\infty} dt e^{i(E-H)t} |\phi_i^+\rangle. \quad (6)$$

B. Application to the $\text{H}_2 + \text{OH}$ reaction

The Hamiltonian for the diatom-diatom system in mass-scaled Jacobi coordinates can be written as^{32,16}

$$H = \frac{1}{2\mu} \sum_{i=1}^3 \left(-\frac{\partial^2}{\partial s_i^2} + \frac{j_i^2}{s_i^2} \right) + V(s_1, s_2, s_3, \theta_1, \theta_2, \phi), \quad (7)$$

where j_1 and j_2 are the rotational angular momenta for H_2 and OH which are coupled to form j_{12} . In the body-fixed frame the orbital angular momentum, j_3 , is represented as $(J-j_{12})^2$, where J is the total angular momentum. In Eq. (7), μ is the mass of the system,

$$\mu = (\mu_1\mu_2\mu_3)^{1/3}, \quad (8)$$

with μ_i ($i=1-3$) being the reduced masses for H_2 , OH , and the system,

$$\begin{aligned} \mu_1 &= \frac{m_{\text{H}} m_{\text{H}}}{m_{\text{H}} + m_{\text{H}}}, \\ \mu_2 &= \frac{m_{\text{H}} m_{\text{O}}}{m_{\text{H}} + m_{\text{O}}}, \\ \mu_3 &= \frac{(m_{\text{H}} + m_{\text{H}})(m_{\text{H}} + m_{\text{O}})}{m_{\text{H}} + m_{\text{H}} + m_{\text{H}} + m_{\text{O}}}. \end{aligned} \quad (9)$$

The mass-scaled coordinates s_i are defined as

$$s_i^2 = \frac{\mu_i}{\mu} R_i^2, \quad (10)$$

where R_i ($i = 1 - 3$) are the bond lengths for H_2 , OH, and the intermolecular distance between the centers of mass of H_2 and OH, respectively.

In the body-fixed frame, coupled total angular momentum eigenfunctions $\mathcal{Y}_{jK}^{JM\epsilon}$ used to expand the TD wave function, are the eigenfunction for J , j_1 , j_2 , j_{12} , and the parity operator.³⁶⁻³⁸ They are defined as³⁹

$$\mathcal{Y}_{jK}^{JM\epsilon} = (1 + \delta_{K0})^{-1/2} \sqrt{\frac{2J+1}{8\pi}} [D_{KM}^J Y_{j_1 j_2}^{j_{12}K} + \epsilon(-1)^{j_1+j_2+j_{12}+J} D_{-KM}^J Y_{j_1 j_2}^{j_{12}-K}], \quad (11)$$

where $D_{K,M}^J$ is the Wigner rotation matrix,⁴⁰ ϵ is the parity of the system, K is the projection of total angular momentum on the body-fixed axis, and $Y_{j_1 j_2}^{j_{12}K}$ is the angular momentum eigenfunction of j_{12} defined as³⁷

$$Y_{j_1 j_2}^{j_{12}K} = \sum_{m_1} \langle j_1 m_1 j_2 K - m_1 | j_{12} K \rangle y_{j_1 m_1} \times (\theta_1, 0)_{j_2, K - m_1}(\theta_2, \phi), \quad (12)$$

and y_{jm} are spherical harmonics. Note in Eq. (11) the restriction $\epsilon(-1)^{j_1+j_2+j_{12}+J} = 1$ partitions the whole rotational basis set into even and odd parities *only for* $K=0$, thus the basis set for $K \neq 0$ is larger than that for $K=0$.

The interaction potential matrix in the angular momentum basis $\mathcal{Y}_{jK}^{JM\epsilon}$ is diagonal in K . It is calculated as^{36,37}

$$\langle \mathcal{Y}_{jK}^{JM\epsilon} | V | \mathcal{Y}_{j'K'}^{JM\epsilon} \rangle = 2\pi \delta_{KK'} \langle Y_{j_1 j_2}^{j_{12}K} | V | Y_{j_1' j_2'}^{j_{12}'K'} \rangle. \quad (13)$$

Thus we can see the potential matrix for even parity is identical to that for odd parity for $K \neq 0$. The centrifugal potential, i.e., the $(J - j_{12})^2$ term in the Hamiltonian shown in Eq. (7), which is not diagonal in K in the BF representation, is given by,^{36,37}

$$\begin{aligned} \langle \mathcal{Y}_{jK}^{JM\epsilon} | (J - j_{12})^2 | \mathcal{Y}_{j'K'}^{JM\epsilon} \rangle \\ = \delta_{j j'} \{ [J(J+1) + j_{12}(j_{12}+1) - 2K^2] \delta_{KK'} \\ - \lambda_{JK}^+ \lambda_{j_{12}K}^+ (1 + \delta_{K0})^{1/2} \delta_{K+1, K'} \\ - \lambda_{JK}^- \lambda_{j_{12}K}^- (1 + \delta_{K1})^{1/2} \delta_{K-1, K'} \} \end{aligned} \quad (14)$$

and the quantity λ is defined as

$$\lambda_{AB}^\pm = [A(A+1) - B(B \pm 1)]^{1/2}. \quad (15)$$

Under the CS approximation, we neglect the coupling between different K in Eq. (14), and calculate the CRP for individual K separately as

$$N(\epsilon, K, E) = \sum_{J \geq K} (2J+1) N(\epsilon, J, K, E). \quad (16)$$

For $K=0$, the different basis sets for even and odd parity result in different values of $N(\epsilon, J, K=0, E)$. However, for $K>0$, the rotational basis set, the interaction potential matrix, as well as the centrifugal potential matrix are the same

for even and odd parities. As a result, $\epsilon = \pm 1$ yield the same value of $N(\epsilon, J, K, E)$ for $K>0$. Thus one has to calculate $N(\epsilon, J, K>0, E)$ for only one parity. The final CRP is the sum of $N(\epsilon, K, E)$,

$$\begin{aligned} N(E) &= \sum_{K, \epsilon} N(\epsilon, K, E) \\ &= \sum_{\epsilon} N(\epsilon, K=0, E) + 2 \sum_{K>0} N(\epsilon=1, K, E). \end{aligned} \quad (17)$$

In order to construct the initial transition state wave packet $|\phi_i^+\rangle$ in Eq. (4), we define two new ‘‘reaction coordinate’’ variables q_1 and q_3 by translating and rotating the s_1 and s_3 axes,^{21,41}

$$\begin{pmatrix} q_1 \\ q_3 \end{pmatrix} = \begin{pmatrix} \cos \chi & \sin \chi \\ -\sin \chi & \cos \chi \end{pmatrix} \begin{pmatrix} s_1 - s_1^0 \\ s_3 - s_3^0 \end{pmatrix}. \quad (18)$$

It can be seen from this equation that we first move the origins of the (s_1, s_3) coordinates to (s_1^0, s_3^0) , then we rotate these two axes by the angle χ . [These coordinates are analogous to collinear reaction coordinates for a triatomic $\text{H}_2 + (\text{OH})$ system.]

The Hamiltonian in Eq. (7) can be written in term of q_1 , s_2 , and q_3 as

$$\begin{aligned} H &= \frac{1}{2\mu} \left(-\frac{\partial^2}{\partial q_1^2} - \frac{\partial^2}{\partial s_2^2} - \frac{\partial^2}{\partial q_3^2} + \frac{j_1^2}{s_1(q_1, q_3, s_1^0, s_3^0)^2} + \frac{j_2^2}{s_2^2} \right. \\ &\quad \left. + \frac{j_3^2}{s_3(q_1, q_3, s_1^0, s_3^0)^2} \right) + V. \end{aligned} \quad (19)$$

By choosing the dividing surface \mathbf{S}_1 at $q_1=0$, we can calculate the ‘‘internal’’ transition states for the other five degrees of freedom by solving for the eigenstates of the 5D Hamiltonian obtained by setting $q_1=0$ in Eq. (19). After constructing the initial wave packets in $(q_1, s_2, q_3, \theta_1, \theta_2, \phi)$ coordinates, we transfer them to the $(s_1, s_2, s_3, \theta_1, \theta_2, \phi)$ coordinates, and propagate them as in the regular wave packet approach. The calculation of the bound states in 5D has been presented in detail in Ref. 42, and the propagation of the 6D wave packet in the diatom-diatom coordinates has been shown in Ref. 3; thus we will not present them again here.

III. RESULTS

A. Numerical parameters

The parameters used in the current study are based on those employed in Ref. 16. We used a total number of 37 sine functions (among them 16 for the interaction region) for the translational coordinate s_3 in a range of $[2.8, 11.0] a_0$. The number of vibrational basis functions used for the reagent OH is 2. A total of 20 vibrational functions are employed for s_1 in the range of $[0.4, 3.8] a_0$ for the reagents H_2 . For the rotational basis, we used $j_{1\text{max}}=14$ for H_2 , $j_{2\text{max}}=16$ for OH. We find that $0 \leq K \leq 9$ converges $N(E)$ adequately up to 0.5 eV. The values of s_1^0 , s_2^0 , and χ which define the transition state surface were carefully chosen to be $3.2 a_0$, $0.6 a_0$, and 33° to minimize the density of states on the dividing surface.

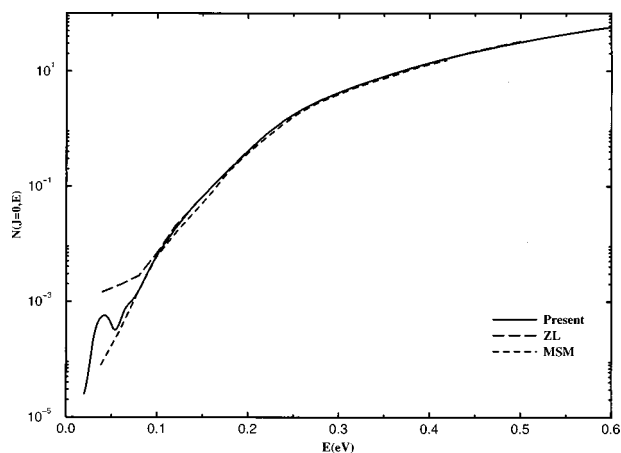


FIG. 1. Cumulative reaction probability $N(J=0,E)$ as a function of energy on a logarithmic scale. Solid line (present results), long-dashed line (Ref. 16), dashed line (Ref. 43).

In addition to the separation of even and odd parities as stated in the previous section, the even and odd rotation states of H_2 are also can be separated. In the present study, we calculated the $N(E)$ only for the even rotation of H_2 . Because the rotation barrier for H_2 in the transition state region on the PES is quite high, the H_2 is constrained, requiring a number of rotational basis functions of either symmetry. Thus the $N(E)$ for the odd rotational manifold of H_2 should be very close to that for the even rotation manifold.

For $K=0-3$, we propagated the wave packets for 9000 a.u. of time to converge the low energy $N(\epsilon,J,K,E)$. For the higher K , because the low energy $N(\epsilon,J,K>3,E)$ are negligible compared to the values given by $K=0-3$, we can converge the non-negligible $N(E)$ in the higher energy region by propagating the wave packets for only 3600 a.u. Even though the TSWP approach has been proven to be very efficient for calculating $N(E)$ for direct reactions, the computation is still extremely time-consuming even for this simplest four-atom reaction. It used about 4 months of CPU time on a single SGI-R10000 processor!

B. The CRP $N(E)$

Figure 1 shows the highly converged $N(J=0,K=0,E)$ with parities summed as a function of energy measured with respect to the ground rovibrational state of reactants. It is very interesting to see that the small peak at very low translational energy found in initial state selected total reaction probability calculation by Zhang and Zhang³ persists quite clearly in $N(J=0,K=0,E)$. This small resonant peak is most likely caused by the unphysical well on the WDSE PES as discussed by Zhang and Zhang. Also shown in Fig. 1 are the CRP results calculated by Manthe *et al.*^{43,44} and that of our previous study in Ref. 16. For high energies, all three calculations agree with each other quite well. However, for very low energies our previous CRP in Ref. 16 obviously was not well converged due to shorter propagation time. Our present CRP for $J=0$ agrees well with that of Manthe *et al.* except that they did not resolve the small peak presumably because the grid they used in normal mode coordinates did not extend to the unphysical well on the PES.^{43,44}

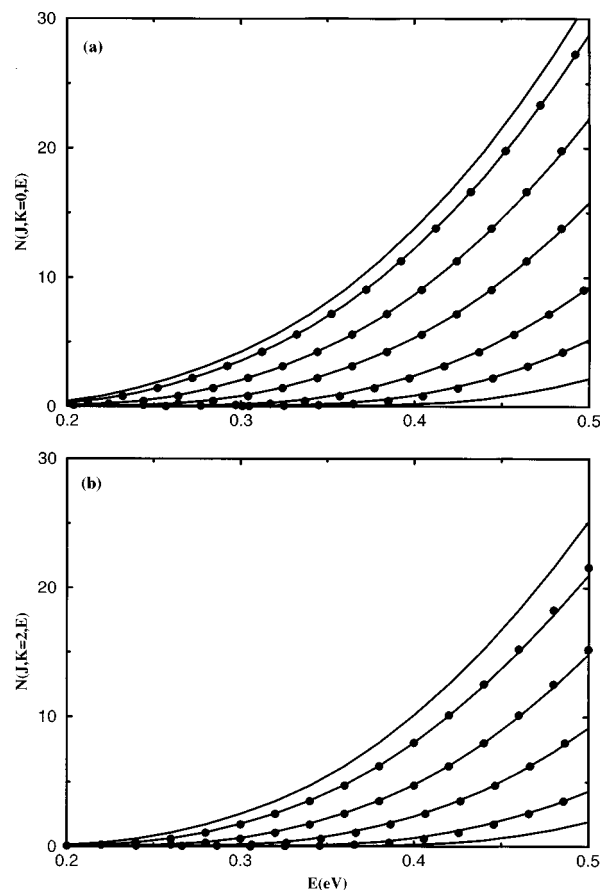


FIG. 2. (a) Cumulative reaction probability $N(J,K=0,E)$ (summed over parities) as a function of energy for $J=0.5, 10, 14, 18, 21, 24$. Solid lines (CS result), solid circles (J-shift result); (b) cumulative reaction probability $N(\epsilon=1, J, K=2, E)$ as a function of energy for $J=2, 7, 12, 16, 20, 23$. Solid lines (CS result), solid circles (J-shift result).

The solid lines in Fig. 2 show the $N(J,K=0,E)$ and $N(J \geq 2, K=2, E)$ for some values of J . As is seen clearly, the J -dependent curves in Fig. 2 are shifted toward higher energy roughly as a quadratic function of J , implying the J -shifting approximation should work here. We also found that the higher J curves for each K , $K=0-9$ can be well approximated by J -shifting from the $N(J=K, K=0-9)$ curve, as shown by the solid circles. The J -shifting values are obtained as

$$N_{J\text{-shifting}}(J>K, K, E) \sim N(J=K, K, E - \Delta E(J, K)), \quad (20)$$

where $\Delta E(J, K) = B^\dagger(J(J+1) - K(K+1))$. The rotational constant B^\dagger of 3.2 cm^{-1} used for a best fit is very close to the *a priori* value of 3.3 cm^{-1} , obtained from $1/(2\mu_3 R_\ddagger^2)$, where μ_3 is the reduced mass for the system in Eq. (9) and R_\ddagger is the intermolecular distance at the saddle point. From Fig. 2 we can see the J -shifting approximation is very good for this reaction, and as we will see later J -shifting also works well for $N(E)$ and the rate constant. We note that a recent initial state selected wave packet study on the $H_2 + CN$ reaction also found that the J -shifting approximation works very well for that reaction.¹³

One should note that we have used the calculated $N(J=K, K)$ ($K=0, 9$) to carry out the J -shifting to obtain the $N(J>K, K)$. However, the approximation used fre-

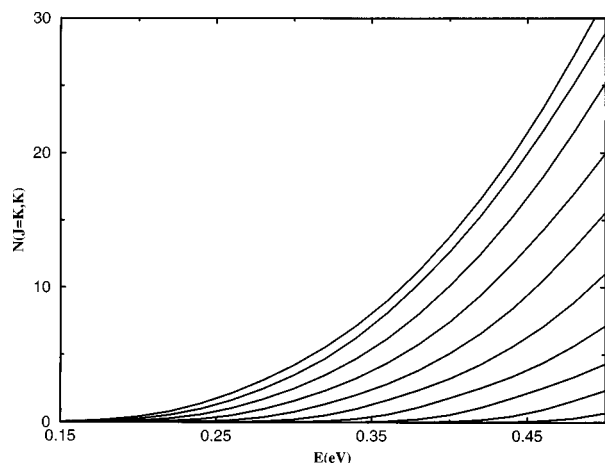


FIG. 3. Cumulative reaction probability $N(J=K, K)$ (summed over parities) and $N(\epsilon=1, J=K, K, E)$ ($1 \leq K \leq 9$) as a function of energy.

quently to evaluate the thermal rate constant from $N(J=0, K=0)$ actually involves both a K-shifting and J-shifting approximation.^{18,1,43} We refer to it here as J- and K-shifting approximation¹ to distinguish the J-shifting approximation procedure we use here. For this reaction we *cannot* fit $N(J=K, K > 0)$ curves in terms of $N(J=0, K=0)$ curves by a simple energy shift. In Fig. 3, we show the $N(J=K, K)$ curves for $K=0-9$. First we found that we cannot fit the $K > 0$ curves from the $K=0$ as well as we did for the J-shifting. Even worse is the fact that we cannot fit the shifts roughly as any quadratic function of K . Thus it is clear that for this reaction, the J-shifting approximation works quite well, while the K-shifting approximation is not very accurate.

This can be understood from the Hamiltonian in Eq. (7) and the angular momentum basis set shown in Eq. (11). Under the CS approximation, the variation of J only changes the value of the effective potential term $[J(J+1) + j_{12}(j_{12} + 1) - 2K^2]$ in Hamiltonian. However, the main effect of the variation of K is not in the $[J(J+1) + j_{12}(j_{12} + 1) - 2K^2]$ term, but in changes of the angular momentum basis set due to the restriction $j_{12} \geq K$ in Eq. (11). Hence the effect of K on the dynamics is much harder to predict than a simple effective potential shift, and can be much stronger than the J effect.²⁰

In Fig. 4, we show $N(K=0, E)$ and $N(\epsilon=1, K=1-9, E)$ [$N(\epsilon=1, K > 0, E) = N(\epsilon=-1, K > 0, E)$ under the CS approximation]. For $K > 3$, we did not try to converge $N(\epsilon=1, K > 3, E)$ if it is less than 0.01. We can see very clearly the shift of $N(\epsilon=1, K, E)$ curves as K increases. The small peak shown in Fig. 1 can still be seen for the first few K .

Figure 5 shows the $N(E)$ summed over all K and parities. It is a very smooth curve, with a small shoulder at $E = 0.05$ eV. Also shown in Fig. 5 is the $N(E)$ obtained by J-shifting which is very close to the CS $N(E)$. This again indicates the J-shifting approximation is good for this reaction.

C. The rate constant

Once one obtains the CRP as a function of energy, $N(E)$, the thermal rate constant is then simply given by its Boltzmann average

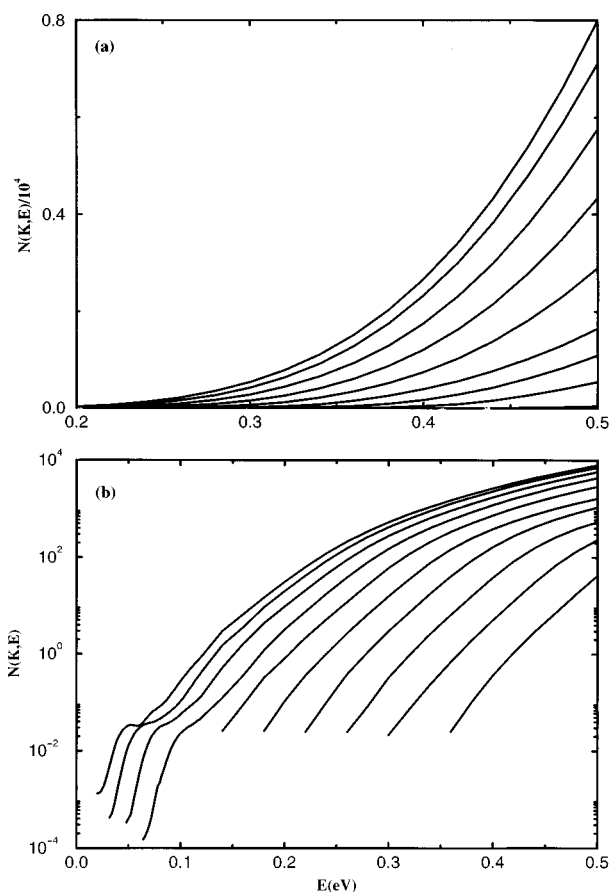


FIG. 4. Cumulative reaction probability $N(K=0, E)$ (summed over parities) and $N(\epsilon=1, K, E)$ ($0 \leq K \leq 9$) as a function of energy. (a) Linear scale; (b) logarithmic scale.

$$k(T) = [2\pi Q_r(T)]^{-1} \int_{-\infty}^{+\infty} dE e^{-E/k_B T} N(E), \quad (21)$$

where $Q_r(T)$ is the reactant partition function (per unit volume).

From $N(E)$ shown in Fig. 5, we can evaluate the thermal rate constants via Eq. (21). Figure 6 and Table I show the main results of this work: the rate constants for the title reaction for the temperature range $300 \text{ K} < T < 800 \text{ K}$ on the WDSE PES under the CS approximation. Also shown in Fig. 6 and Table I are the rate constant calculated from the J-shifting $N(E)$ shown in Fig. 5. For high temperatures, the agreement between the CS result and the J-shifting result is essentially perfect; for $T=800 \text{ K}$, the difference is 2%. For low temperatures, the error is slightly larger, for $T=300 \text{ K}$ the J-shifting result is smaller than the CS result by 10%. Tuning of the B^\ddagger constant for the shifting should make the agreement even better.

In Fig. 6 and Table I, we also show the rate constants calculated from $N(J=0, E)$ (shown in Fig. 1) by using the J- and K-shifting approximation,^{18,43}

$$k_{JK\text{-shifting}}(E) \approx [2\pi Q_r(T)]^{-1} Q_{\text{rot}}^\ddagger \times \int_{-\infty}^{\infty} dE e^{-E/k_B T} N(J=0, E), \quad (22)$$

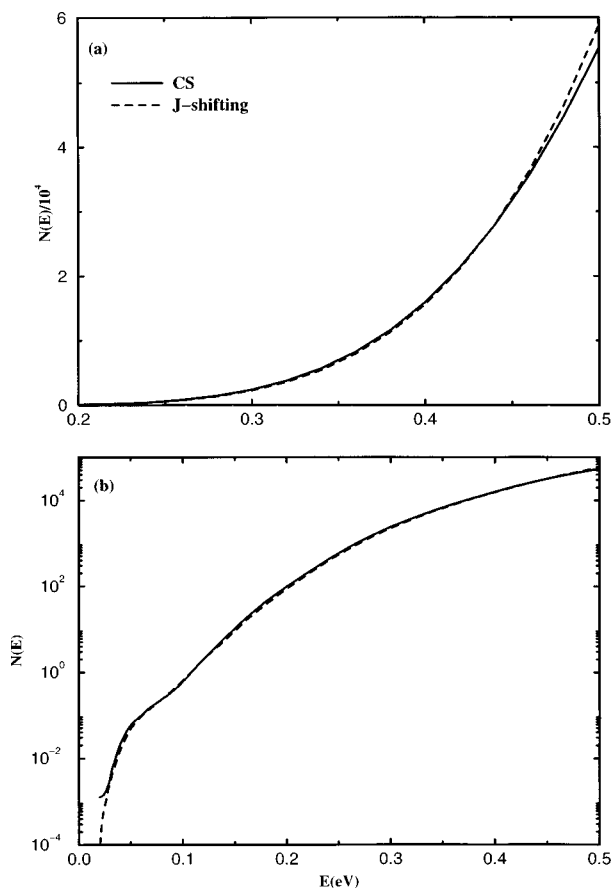


FIG. 5. Cumulative reaction probability $N(E)$ for title reaction as a function of energy, solid lines (CS result), dashed lines (J-shifting result): (a) Linear scale; (b) logarithmic scale.

where $Q_{\text{rot}}^{\ddagger}$ is the rotational partition function for the H_2OH complex and can be well approximated by the classical expression,

$$Q_{\text{rot}}^{\ddagger} = \sqrt{8 \pi (k_B T)^3 I_A^{\ddagger} I_B^{\ddagger} I_C^{\ddagger}} \quad (23)$$

where I_A^{\ddagger} , I_B^{\ddagger} , and I_C^{\ddagger} are the three principle moments of inertia for the H_2OH complex in the transition state geometry (On the WDSE PES, $I_A^{\ddagger} = 4079$ a.u., $I_B^{\ddagger} = 37520$ a.u., $I_C^{\ddagger} = 41599$ a.u.). Since one only uses $N(J=0, K=0, E)$ to calculate the rate constant, one has to make shifts for J (J-shifting) as well as for K (K-shifting) to get the CRP for all the K and J . As we can see from Fig. 6 that the J- and K-shifting rate constants have the same trend as the CS result, but are consistently larger than the accurate rates by a factor of 1.6 for all the temperatures considered here. As we have mentioned in the Introduction, the CS approximation is within around 20%–25% of the accurate thermal rate constant for some atom-diatom reactions, and we would expect

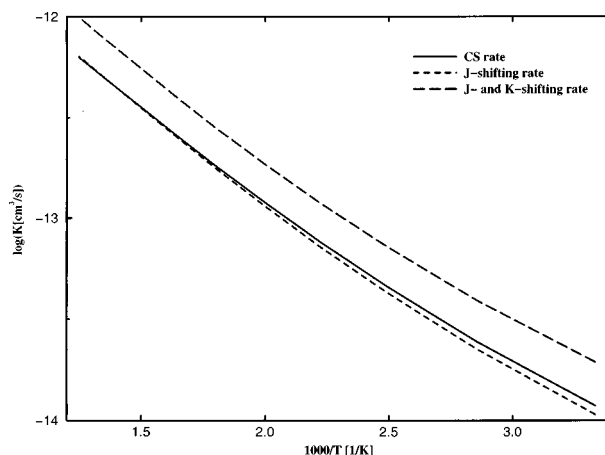


FIG. 6. Rate constant of the $\text{H}_2 + \text{OH} \rightarrow \text{H}_2\text{O} + \text{H}$ reaction. solid line (present CS results), dashed line (present J-shifting values), and long-dashed line (present J- and K-shifting values).

it is within this accuracy for this diatom-diatom reaction. Thus the J- and K-shifting approximation overestimates the rate constant by at least 40% for the entire temperature region. Also the comparison among the CS result, the J-shifting result, and the J- and K-shifting result shows very clearly that the K-shifting approximation causes the major part of the discrepancy between the J- and K-shifting rate constant and the CS rate constant, since the J-shifting result is in very good agreement with the CS result.

Let us now compare our CS rate constants with experimental values.⁴⁵ In Fig. 7, we can see the trend of rates of our calculation is rather different from that of experiment. For low temperatures the theoretical rates are higher than the experimental values. For $T=300$ K, the theoretical rate is higher than the experimental rate by 80%. However, the increase of theoretical rate constant with temperature is significantly slower than that for experiment. As a result, for temperatures higher than 500 K, the theoretical rate constant is lower than the experimental one. We believe that the CS approximation cannot introduce such a large error in rate constant. Thus the discrepancy between theory and experiment is probably due to inaccuracies in the potential energy surface. An improvement of this surface appears to be necessary in order to obtain a quantitative description of the reaction.

Finally we compare our accurate rate constants with other theoretical results. Because the cumulative reaction probabilities for $J=0$ by Manthe, Seideman, and Miller,^{43,44} by Wang and Bowman,⁴⁶ and by Pogrebnya, Echave, and Clary⁴⁷ are quite close to the present CRP for $J=0$, their rate constants obtained by the J- and K-shifting approximation should be close to the present J- and K-shifting results. Thus

TABLE I. Thermal rate constants $k(T)$ (10^{-14} cm^3/s) as a function of temperature for the $\text{H}_2 + \text{OH}$ reaction.

T(K)	300	350	400	450	500	550	600	650	700	750	800
CS rate	1.20	2.44	4.53	7.66	12.0	17.6	24.5	32.5	41.7	51.7	62.4
J-shifting rate	1.08	2.26	4.24	7.26	11.5	17.1	24.0	32.1	41.6	52.0	63.2
J- and K-shifting rate	1.94	3.91	7.14	11.9	18.6	27.1	37.8	50.4	65.0	81.2	99.1

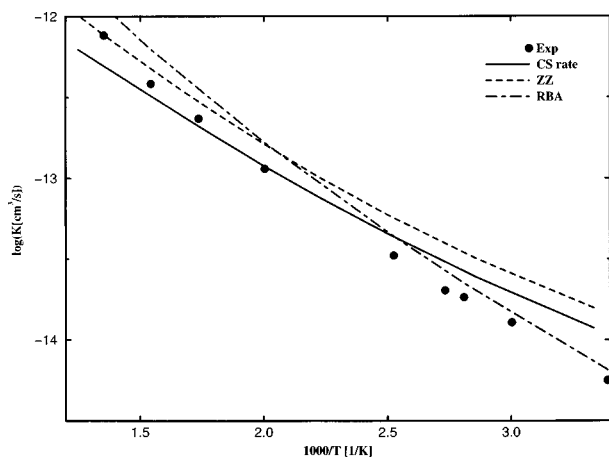


FIG. 7. Comparison of the present CS rate constant with the experimental and other theoretical results. Solid circles (experimental values, Ref. 45), solid line (present CS results), dot-dashed line (Ref. 3), and dashed line (Ref. 32).

we do not show their results on Fig. 7. First, let us compare our CS rate constant with the initial state-specific rate constants for $\text{H}_2(\nu=0, j=0)+\text{OH}(\nu=0, j=0)$, $k_{\text{ground}}(T)$.³ Note that the k_{ground} here is slightly different from that shown in Ref. 3 by Zhang and Zhang, because here we used

$$Q_{\text{OH}}^{\text{elec}}(T) = 1 + e^{-\Delta E_{\text{elec}}/kT}, \quad (24)$$

with $\Delta E_{\text{elec}} = 140 \text{ cm}^{-1}$,

for the OH electronic partition function, while Zhang and Zhang simply used 2. As can be seen from the figure, the k_{ground} is quite substantially larger than the current CS rate constant, by 30% at $T=300 \text{ K}$ and 60% at $T=800 \text{ K}$. Because the CS approximation is used in both calculations, we tend to believe the difference comes mainly from the fact that the k_{ground} does not include the effects of rotations of reagents on the rate constant. The significant difference between the CS rate constant and k_{ground} indicates that initial rotational excitation is quite important to the thermal rate constant.

Finally, we see that the rigid bender approximation (RBA) result of Clary³² lies below our calculated results at low temperatures but is above at higher temperatures. The better agreement between the experiment and RBA is likely to be fortuitous as discussed by Manthe *et al.*⁴⁴

IV. CONCLUSIONS

The CRP $N(E)$ for the prototypical four-atom reaction H_2+OH has been calculated on the WDSE surface using only the CS approximation. The calculation, with all J summed, is much more computationally demanding than that for $N(E)$ ($J=0$), and once again demonstrates that the TSWP approach developed by Zhang and Light allows for very efficient calculations of the CRP for direct reactions with barriers in the transition state region. The rate constant for the title reaction is then calculated from the $N(E)$. Comparison shows significant differences between the present

rate constant and the experimental results, indicating the PES should be improved in order to obtain a truly quantitative description of the reaction.

Our calculation also show that the J-shifting approximation in which we approximate the $N(J>K, K)$ by shifting $N(J=K, K)$ works very well for this reaction. On the other hand, the J- and K-shifting approximation in which we calculate the rate constant solely from $N(E)$ ($J=0$) significantly overestimates the rate constant, indicating the K-shifting approximation is not good for this reaction. More tests on other reactions are highly desirable to verify if this is a general result for four-atom reactions. However, even if only the J-shifting approximation is good, it still can reduce the computational time by a factor of 5–10.

It is found that the full CS rate constant is quite significantly smaller than the rate constant calculated for ground state reagents only. This implies that initial rotational excitation of reagents is important to the thermal rate constant, and that overall it reduces the thermal rate constant for this reaction.

Since the CS approximation has been never tested for any four-atom reaction, future study will need to address the question of how accurate the CS approximation is for this four-atom reaction. The CS approximation has also been applied frequently in the initial state selected wave packet approach to calculate the total cross section and rate constant for some initial states. Thus it will be extremely important to carry out such a test.

ACKNOWLEDGMENTS

This work is supported in part by the Academic Research Grant RP970632, National University of Singapore, and the NSF Grant CHE-9634440. D. H. Zhang would like to thank Dr. Uwe Manthe for very helpful discussions during the course of this work.

- ¹D. C. Clary, *J. Phys. Chem.* **98**, 10678 (1994).
- ²J. M. Bowman and G. C. Schatz, *Annu. Rev. Phys. Chem.* **46**, 169 (1996).
- ³D. H. Zhang and J. Z. H. Zhang, *J. Chem. Phys.* **101**, 1146 (1994).
- ⁴D. Neuhauser, *J. Chem. Phys.* **100**, 9272 (1994).
- ⁵D. H. Zhang and J. Z. H. Zhang, in *Dynamics of Molecules and Chemical Reactions*, edited by R. E. Wyatt and J. Z. H. Zhang (Marcel Dekker, New York, 1996).
- ⁶D. H. Zhang and J. C. Light, *J. Chem. Phys.* **104**, 4544 (1996).
- ⁷W. Zhu, J. Dai, J. Z. H. Zhang, and D. H. Zhang, *J. Chem. Phys.* **105**, 4881 (1996).
- ⁸D. H. Zhang and J. C. Light, *J. Chem. Phys.* **105**, 1291 (1996).
- ⁹D. H. Zhang and J. Z. H. Zhang, *Chem. Phys. Lett.* **232**, 370 (1995).
- ¹⁰D. H. Zhang, J. Z. H. Zhang, Y. C. Zhang, D. Wang, and Q. Zhang, *J. Chem. Phys.* **102**, 7400 (1995).
- ¹¹D. H. Zhang and J. C. Light, *J. Chem. Soc., Faraday Trans.* **93**, 691 (1997).
- ¹²D. H. Zhang and J. Z. H. Zhang, *J. Chem. Phys.* **103**, 6512 (1995).
- ¹³W. Zhu, J. Z. H. Zhang, Y. C. Zhang, Y. B. Zhang, L. X. Zhan, S. L. Zhang, and D. H. Zhang, *J. Chem. Phys.* **108**, 3509 (1998).
- ¹⁴U. Manthe and W. H. Miller, *J. Chem. Phys.* **99**, 3411 (1993).
- ¹⁵U. Manthe, T. Seideman, and W. H. Miller, *J. Chem. Phys.* **99**, 10 078 (1993).
- ¹⁶D. H. Zhang and J. C. Light, *J. Chem. Phys.* **106**, 551 (1997).
- ¹⁷D. H. Zhang and J. C. Light, *Faraday Discuss.* (submitted).
- ¹⁸Q. Sun, J. M. Bowman, G. C. Schatz, J. R. Sharp, and J. N. L. Connor, *J. Chem. Phys.* **92**, 1677 (1990).
- ¹⁹J. M. Bowman, *J. Phys. Chem.* **95**, 4960 (1991).
- ²⁰O. Roncero, D. Caloto, K. C. Janda, and N. Halberstadt, *J. Chem. Phys.* **107**, 1406 (1997).
- ²¹D. H. Zhang and J. C. Light, *J. Chem. Phys.* **104**, 6184 (1996).

- ²²T. J. Park and J. C. Light, *J. Chem. Phys.* **85**, 5870 (1986).
²³T. J. Park and J. C. Light, *J. Chem. Phys.* **88**, 4897 (1988).
²⁴D. Brown and J. C. Light, *J. Chem. Phys.* **97**, 5465 (1992).
²⁵W. H. Thompson and W. H. Miller, *J. Chem. Phys.* **106**, 142 (1997).
²⁶H. Wang, W. H. Thompson, and W. H. Miller, *J. Chem. Phys.* **107**, 7194 (1997).
²⁷T. Seideman and W. H. Miller, *J. Chem. Phys.* **97**, 2499 (1992).
²⁸R. T. Pack, *J. Chem. Phys.* **60**, 633 (1974).
²⁹P. McGuire and D. J. Kouri, *J. Chem. Phys.* **60**, 2488 (1974).
³⁰S. P. Walch and J. T. H. Dunning, *J. Chem. Phys.* **72**, 1303 (1980).
³¹G. C. Schatz and H. Elgersma, *Chem. Phys. Lett.* **73**, 21 (1980).
³²D. C. Clary, *J. Chem. Phys.* **95**, 7298 (1991).
³³A. Aguado, M. Paniagua, M. Lara, and O. Roncero, *J. Chem. Phys.* **107**, 10085 (1997).
³⁴W. H. Miller, S. D. Schwartz, and J. W. Tromp, *J. Chem. Phys.* **79**, 4889 (1983).
³⁵T. Seideman and W. H. Miller, *J. Chem. Phys.* **95**, 1768 (1991).
³⁶M. H. Alexander and A. P. DePristo, *J. Chem. Phys.* **66**, 2166 (1977).
³⁷D. H. Zhang and J. Z. H. Zhang, *J. Chem. Phys.* **99**, 6624 (1993).
³⁸D. H. Zhang and J. Z. H. Zhang, *J. Chem. Phys.* **99**, 5615 (1993).
³⁹D. H. Zhang and J. Z. H. Zhang, *J. Chem. Phys.* **101**, 1146 (1994).
⁴⁰M. E. Rose, *Elementary Theory of Angular Momentum* (Wiley, New York, 1957).
⁴¹J. M. Bowman, J. Zuniga, and A. Wierzbicki, *J. Chem. Phys.* **90**, 2708 (1989).
⁴²D. H. Zhang, Q. Wu, J. Z. H. Zhang, M. Dirke, and Z. Bačić, *J. Chem. Phys.* **102**, 2315 (1995).
⁴³U. Manthe, T. Seideman, and W. H. Miller, *J. Chem. Phys.* **99**, 10078 (1993).
⁴⁴U. Manthe, T. Seideman, and W. H. Miller, *J. Chem. Phys.* **101**, 4759 (1994).
⁴⁵F. P. Tully and A. R. Ravishankara, *J. Phys. Chem.* **84**, 3126 (1980).
⁴⁶D. Wang and J. M. Bowman, *J. Chem. Phys.* **96**, 8906 (1992).
⁴⁷S. K. Pogrebnya, J. Echave, and D. C. Clary, *J. Chem. Phys.* **107**, 8975 (1997).